Fast and Accurate Analysis of Reflector Antennas with Struts and Satellite Platform Scattering

Niels Vesterdal, Oscar Borries, Min Zhou, Knud Pontoppidan, Erik Jørgensen
TICRA, DK-1201 Copenhagen, Denmark

***Abstract*—This paper presents two methods related to modelling of reflector antenna struts and surrounding structural features such as satellite platforms. One method is a MoM-based strut model and represents an improvement of an existing PO-based model, thus enabling analysis of concave cross sections and dielectric materials, while generally speeding up the analysis. The other is a full-wave higher-order MLFMM which offers a significant reduction of the required computational resources compared to commonly available lower-order MLFMM. The methods are demonstrated on two reflector antenna systems including struts as well as a large satellite platform. Both methods exhibit significant reduction of required computation time and resources.**

***Index Terms*—Reflector antenna, Struts, Satellite platform, Higher-Order MLFMM**

I. Introduction

The Physical Optics (PO) and Physical Theory of Diffraction (PTD) is used extensively for reflector antenna analysis and design. An inherent part of any successful reflector antenna design must, however, take the presence of struts and other structures, which do not lend themselves well to the approximations inherent in the PO/PTD computational model, into account. For decades, methods for strut analysis have thus been an important part of commercially available software packages, e.g., GRASP that for several years has offered a fast analytically-based method for circular struts and a PO-based method for struts of more general polygonal cross section. Being based on PO, this method is limited to perfect electric conductors (PEC) of convex cross section. In addition to modelling of struts, the scattering from structural surroundings such as satellite platforms is of importance. This is particularly relevant when defining antenna locations on the very limited space available on most satellite platforms.

The research presented in this paper has focused on further advancing the analysis capabilities, not only in the regime of the antenna itself, but also extending this to include surrounding mounting structures such as satellite platforms. As to the former, a computational model for strut analysis based on a 2-dimensional Method of Moments (2D MoM) has been developed and recently became available in GRASP. This method removes the above-mentioned limitations of the PO-based method and furthermore facilitates modelling of dielectric struts. As to the latter a newly developed Higher-Order Multi-Level Fast Multipole Method (HO-MLFMM) [1], incorporating very high order Legendre basis functions [2], offers fast and accurate modelling of large, complex structures, e.g., satellite platforms.

This paper will briefly outline the principles behind the new MoM-based strut analysis, whereas the details on the HO-MLFMM method are omitted but can be found in [1]. Demonstrations of the capabilities offered by these methods are subsequently given by means of two examples of application. First, the MoM-based strut analysis and HO-MLFMM are demonstrated for an antenna with varying types of struts, illustrating the increased flexibility of the strut analysis in terms of geometries and materials as well as the speed and accuracy of both methods. Second, a dual reflector antenna system modelled from the Olympus Satellite [3] is analysed using PO/PTD and HO-MLFMM. The impact of scattering from the Olympus satellite platform is subsequently modelled demonstrating a typical application where the powerful capabilities of HO-MLFMM can be applied.

II. MoM-Based Modelling of Struts with Arbitrary Cross Section

The newly developed MoM-based method for struts uses a 2D MoM formulation to characterise the cross-sectional geometry of the strut. Using this, the strut currents are calculated repeatedly in several cross sections along the longitudinal dimension of the strut. When all currents are calculated they are integrated along the finite extent of the strut and the scattered field is evaluated. The necessary number of current cross sections is determined using an auto-convergence procedure and a selected convergence level.

The 2D MoM model is based on the assumption of an infinitely long cylinder of general cross section being illuminated by a plane wave with incidence angle θ^i. This two-dimensional case is easily derived from the more general three-dimensional case, e.g., as detailed in [4]. The electric and magnetic currents on the strut are expanded using higher-order hierarchical Legendre basis functions [2]. Since the problem is two-dimensional the functions simplify as compared to the three-dimensional case. The currents are expressed as

$$\mathbf{X}(\vec{\rho}) = \sum_{m=0}^{M^u} a_m^u \mathbf{B}_m^u + \sum_{n=0}^{M^u-1} a_n^v \mathbf{B}_n^v, \tag{1}$$

where $\mathbf{X}$ is the electric or magnetic current. The quantities a_m^u and a_n^v are expansion coefficients of the vector basis functions

$$\mathbf{B}_m^u(u) = \frac{\vec{u}}{|\vec{u}|}\tilde{P}_m(u), \quad \mathbf{B}_n^v(u) = \frac{\hat{z}}{|\vec{u}|}P_n(u), \tag{2}$$

in the cross-sectional plane and along the cylinder axis, respectively. The vector $\vec{u} = \frac{\partial}{\partial u}\vec{\rho}(u)$ with $\vec{\rho}(u)$ being the cross-sectional coordinate and u is a parametric coordinate in the interval $[-1, 1]$. Note that while $\hat{z}$ is the unit vector along the cylinder axis, $\vec{u}$ is not a unit vector. The polynomials $P_n(u)$ and $\tilde{P}_m(u)$ are, respectively, Legendre and modified Legendre polynomials [2]. For each incidence angle the associated expansion coefficients can be found by solving the set of linear equations given by

$$[I(\theta^i)] = [Z(\theta^i)]^{-1}[V(\theta^i)], \tag{3}$$

where $[Z(\theta^i)]$ is the MoM impedance matrix for incidence angle θ^i and $[V(\theta^i)]$ holds the expansion coefficients of the incident plane wave. In the case of closed strut cross sections, the Combined Field Integral Equation is used in order to avoid problems with interior resonances in the Electric Field Integral Equation.

By evaluating the direction of the incident field, the appropriate 2D MoM problem can in principle be formed. In practice this is, however, not an effective procedure since it requires the MoM matrix to be calculated and inverted for every incidence angle. Instead a fixed set of incidence angles θ^k are selected and the associated MoM matrices $[Z(\theta^k)]$ are LU-decomposed and stored. The use of interpolation in θ^i renders the necessary number of stored MoM matrices fairly moderate.

With the cross-sectional dimension thus taken care of, the currents can be calculated along the entire strut by applying the appropriate incident field corresponding to a particular location on the strut surface. Defining this point in cylindrical coordinates $(\vec{\rho}_0, z_0)$ of the local strut coordinate system, the current calculation proceeds as follows:

- Evaluate the incident field at the strut cross section at z_0 and calculate the direction of incidence θ^i using the Poynting vector.
- Select a set of pre-defined θ^k close to θ^i and calculate $[V(\theta^k)]$.
- Solve for the currents' expansion coefficients $[I(\theta^k)]$ using the stored impedance matrices $[Z(\theta^k)]$.
- Interpolate among the calculated $[I(\theta^k)]$ and find the currents on the z_0 cross section.
- Extract the strut current in the point $(\vec{\rho}_0, z_0)$.

III. Reflector with 3 Struts

The MoM-based algorithm for strut calculations is demonstrated by an example of a single reflector antenna with three struts. The antenna is depicted in Figure 1 where also the strut cross sections are illustrated. Four specific cases, 1a-1d, are defined, one without struts (1a), two with PEC struts (1b,c), and lastly a case of dielectric struts (1d). The PEC struts differ by being either convex (1b) and concave (1c), respectively. The reflector is a parabolic reflector with diameter $D = 0.65$ m and focal length $f = 0.325$ m and is analysed at 30.0 GHz. It thus represents a typical antenna size and frequency encountered among present-day VSAT antennas, e.g., in mobile satellite communications in the Ka-band. Further details on the four cases are listed in Table I.

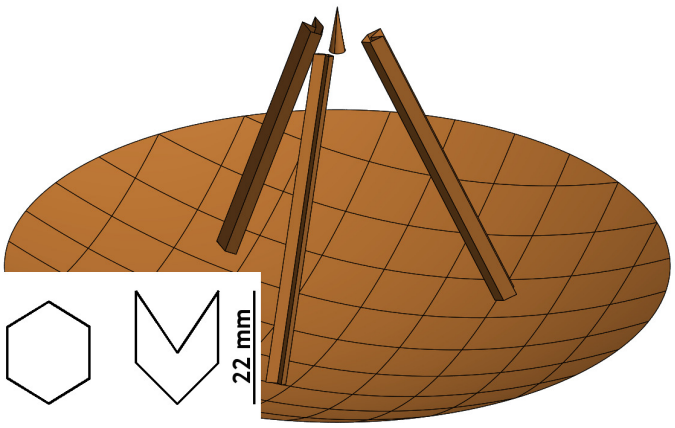

Fig. 1. Example of the reflector antenna with 3 struts, shown with the concave PEC struts. The convex and concave strut cross sections are shown in the lower left corner.

For the analysis of these cases, a total of four computational methods will be employed. The standard PO/PTD [5] is employed on the main reflector in combination with the respective PO-based and MoM-based struts analysis algorithms. Unrelated to these methods, the HO-MLFMM is also used on the entire antenna. Thus three different computational models result:

- PO/PTD + PO (PO/PTD on main reflector and PO-based strut model). Has been commercially available in GRASP for several years.
- PO/PTD + MoM (PO/PTD on main reflector and MoM-based strut model). Has recently been released in GRASP.
- HO-MLFMM. Not yet released.

It is noted that when applying the PO/PTD with the strut analysis algorithms the recommended standard procedure is used as detailed in [5]. For cases 1c and 1d only the MoM-based strut method is used since these configurations can not be analysed with the PO-based method. As reference solution, the standard commercially available higher-order MoM solution of GRASP [5] is used for cases 1a-1c. However, it has not been possible to analyse case 1d using MoM due to the high computational cost. In this case a highly over-discretised HO-MLFMM solution is used as reference in stead. In Table II a summary of the computations using the 3 methods are listed. In this table the quantity

$$\Delta_{RMS} = \frac{\sqrt{\sum_{i=1}^{N_S} |\vec{E}_i - \vec{E}_{ref,i}|^2}}{\sqrt{\sum_{i=1}^{N_S} |\vec{E}_{ref,i}|^2}}, \tag{4}$$

denotes the relative RMS value of the deviation of the calculated far field $\vec{E}$ from the reference solution $\vec{E}_{ref}$ with N_S being the number of far-field samples. Since the models using the PO-based methods (i.e., either on the reflector or struts) are entirely different from the integral-equation-based, i.e., MoM or HO-MLFMM, they can obviously not be expected

TABLE I
SUMMARY OF STRUT CHARACTERISTICS FOR THE FOUR DIFFERENT CASES

Case	Number of struts	Strut material	Strut Shape
1a	0	N.A.	N.A.
1b	3	PEC	Convex
1c	3	PEC	Concave
1d	3	Dielectric, $\epsilon_r = 2.0$, $\tan\delta = 0.02$	Convex

TABLE II
SUMMARY OF CALCULATIONS OF REFLECTOR WITH 3 STRUTS (INTEL CORE I7 @ 2.60GHZ)

Case	Method	Δ_{RMS}	Time	Memory
1a	PO/PTD	0.00363	0.7s.	$<$ 20 MB
	HO-MLFMM	0.00023	2m 58s.	753 MB
1b	PO/PTD + PO	0.03149	21m 43s.	20 MB
	PO/PTD + MoM	0.01837	24.4s.	68 MB
	HO-MLFMM	0.00279	4m 15s.	1.02 GB
1c	PO/PTD + MoM	0.02967	29.3s.	103 MB
	HO-MLFMM	0.00358	4m 24s.	1.14 GB
1d	PO/PTD + MoM	0.01459	40.4s.	133 MB
	HO-MLFMM	0.00298	13m 32s.	3.29 GB

to converge to the same solution. Hence the term "error" is intentionally avoided when comparing these two types of methods. However, when comparing the HO-MLFMM with the reference, Δ_{RMS} may be interpreted as an error due to the selected discretisation and HO-MLFMM accuracy parameters. The computation time and memory consumption of the various methods are also listed in Table II.

Examples of the radiation patterns for the four cases are shown in Figure 2 in the interval $\theta \in [-45^o, 45^o]$. Considering case 1a, it is immediately seen that both methods agree very well with the reference MoM solution which is also seen from Table II. This case is of course very well suited for PO/PTD and consequently this method is much more efficient than the HO-MLFMM, using only 0.7 seconds compared to more than 3 minutes for HO-MLFMM. Having said this it is, nonetheless, clear that the computational resources required by HO-MLFMM represent a vast reduction as compared to the MoM reference.

As for case 1b, the MoM-based strut method is seen to be closer to the reference than the PO-based one. This is also seen from the obtained Δ_{RMS} which is significantly reduced. Thus a good agreement between the two is seen down to a level of roughly 30 dB below peak, whereas the results for the PO-based strut method start to deviate already around 25 dB below peak. Regarding the computation time, it is noted that the MoM-based strut method is significantly faster than the PO-based one, using only 24 seconds. The HO-MLFMM solution is very close to the MoM reference and uses a little more then 4 minutes.

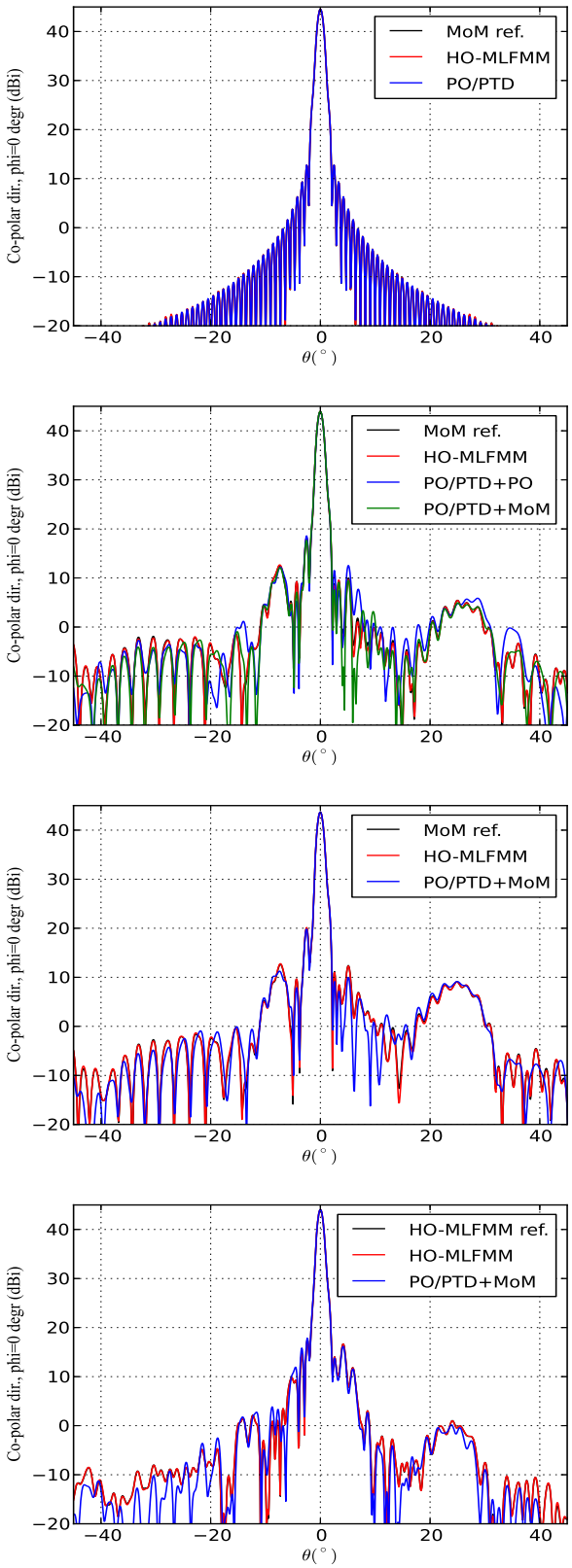

Fig. 2. Calculated radiation patterns of the reflector antenna in Figure 1 equipped with different types of struts. Cases 1a through 1d are shown from top to bottom.

Cases 1c and 1d can not be analysed with the PO-based strut method. Comparison of the MoM-based strut method with the reference shows a similarly good agreement for 1c as was the case for 1b and the computation time using the MoM-based strut method is close to that of case 1b. For the dielectric case, 1d, a similar level of agreement results. Lastly it is noted that the MoM-based strut method handles the cases 1b through 1d using from 20 to 40 seconds, whereas the HO-MLFMM requires slightly more than 4 minutes for the PEC cases and about 13.5 minutes for the dielectric case. For all cases, it is seen that the HO-MLFMM is almost indistinguishable from the respective MoM and over-discretised HO-MLFMM reference solutions.

IV. Dual Reflector System on Satellite Platform

A further example demonstrating the general capabilities of the HO-MLFMM is given here in the form of a television broadcast antenna system operating at 12/18 GHz on the Olympus satellite [3]. The antenna is an offset dual reflector antenna consisting of a slightly elliptical sub reflector, about 0.6 m across, and a highly elliptical main reflector, 0.8 m and 1.94 m across, in the two respective planes. In Figure 3 this antenna system, denoted TVB1, and the satellite platform are shown. As a first case, denoted 2a, the antenna alone is analysed at its down-link frequency of 12 GHz. The resulting patterns are calculated using HO-MLFMM and validated by comparison with results from both the standard PO/PTD and reference MoM solutions and these results are shown in the top of Figure 4 for $\theta \in [-60^{\circ}, 60^{\circ}]$. The patterns are seen to be in very good agreement down to a level of at least 50 dB below peak. Indeed the MoM and HO-MLFMM solutions agree to an even lower level. The PO/PTD and HO-MLFMM methods use, respectively, about 16 seconds and 1 minute. Additional data on the size of the problems and other computational characteristics are summarised in Table III and IV. In Table III the numbers of unknowns relate to the present use of higher-order basis functions. As a means of comparison with low-order implementations, the equivalent numbers of unknowns for an RWG implementation [6] are also listed, being approximated as roughly 4-5 times higher than a higher-order method [2].

Case 2a is now compared to the case where scattering from the satellite platform is included, henceforth denoted case 2b. In the bottom of Figure 4 the respective patterns can be seen, also analysed at 12 GHz and shown for $\theta \in [-180^{\circ}, 180^{\circ}]$, thus allowing the impact on the TVB1 radiation characteristics to be evaluated. The patterns for the two cases are seen to diverge at a level of roughly 40 dB below peak which indicates that platform scattering only has little impact on the TVB1 performance. Using the HO-MLFMM on this problem requires roughly 63 GB of memory and a little more than 2 hours of computation time.

The fact that MLFMM in general yields significant reductions of memory requirements compared to the corresponding MoM solution is well known. The present HO-MLFMM, being based on higher-order basis functions, has previously been demonstrated to be superior to conventional low-order MLFMM [1]. The reduction in memory consumption associated with the presently discussed cases is listed in Table V. Depending on the case the HO-MLFMM is seen to reduce the memory consumptions to fractions in the interval from 0.04% to 1.9%.

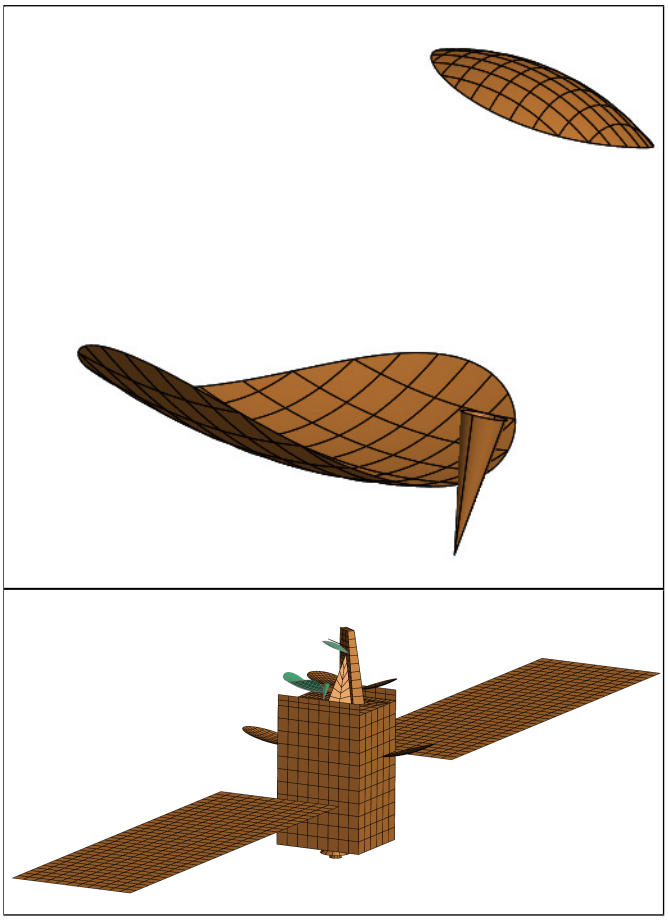

Fig. 3. Dual reflector antenna system. Top: Antenna alone. Bottom: Antenna (shown in green) situated on a model of the Olympus satellite platform.

V. Conclusion

Two recent developments at TICRA have been demonstrated, including a recently released MoM-based strut analysis method and a HO-MLFMM. The former demonstrated increased accuracy and flexibility compared to a previously existing method based on PO which has been commercially available for several years. This has enabled analysis of more general strut shapes with concave cross section as well as dielectric struts using very low run time and memory. The HO-MLFMM offers fast and accurate analysis of large structures without compromising the accuracy of full-wave methods.

By way of examples, the capabilities of these methods have been demonstrated, firstly by considering a Ka-band reflector antenna with different types of struts and secondly a 12 GHz television broadcast antenna situated on the Olympus satellite. In the first example four antenna/strut cases were

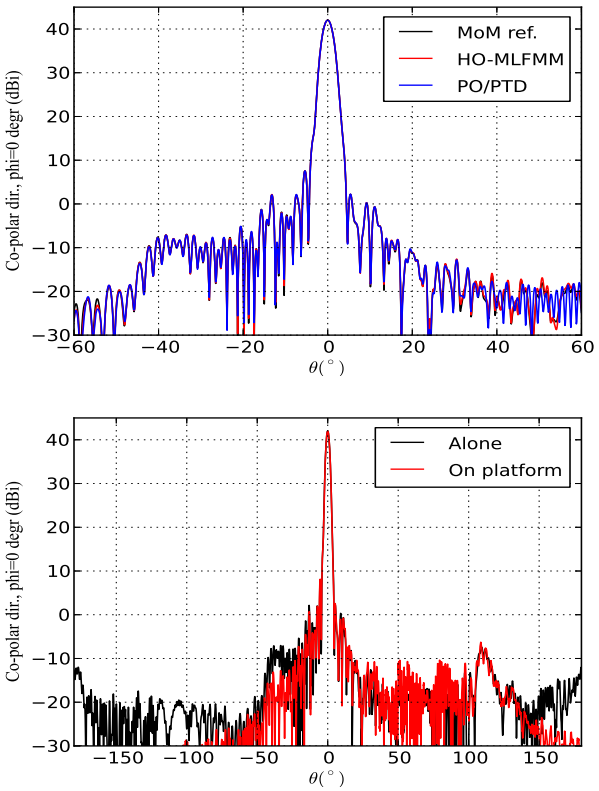

Fig. 4. Calculated radiation patterns of the TVB-1 antenna from the Olympus satellite. Top: antenna alone analysed with PO/PTD and HO-MLFMM. Bottom: HO-MLFMM analysis of antenna alone and on platform.

TABLE III
SUMMARY OF THE CASES WITH THE TVB1 DUAL REFLECTOR ANTENNA SYSTEM ON OLYMPUS

Case	Antenna location	Problem size	HO-unknowns	Equiv. RWG unknowns
2a	Alone	2683 λ^2	101762	$\sim$ 0.5 mio.
2b	On platform	167014 λ^2	4384717	$\sim$ 20 mio.

TABLE IV
SUMMARY OF CALCULATIONS OF TVB1 DUAL REFLECTOR ANTENNA SYSTEM FROM THE OLYMPUS SATELLITE (DUAL XEON E5-2690 @ 2.90GHZ)

Case	Method	Δ_{RMS}	Time	Memory
2a	PO/PTD	0.00708	16.2s.	21 MB
	HO-MLFMM	0.00239	1m 5s.	681 MB
2b	HO-MLFMM	0.00262	2h 17m.	62.6 GB

analysed including dielectric struts and struts with concave cross section. Through this, the added flexibility, increase of speed, as well as enhanced accuracy, as compared to the PO-based method, were demonstrated. The HO-MLFMM was also applied to these cases and testified to the efficiency that it provides. With the second example of the Olympus satellite antenna and platform, the capabilities of the HO-MLFMM were further corroborated requiring merely about 1 minute for the antenna alone and a little more than two hours for the entire satellite platform.

TABLE V
SUMMARY OF THE MEMORY REQUIREMENTS USING HO-MLFMM AND OF THE CORRESPONDING MOM OF STANDARD GRASP

Case	HO-MLFMM	MoM ref.	Memory ratio
1a	755 MB	68 GB	$11.11 \cdot 10^{-3}$
1b	1.02 GB	94 GB	$10.85 \cdot 10^{-3}$
1c	1.14 GB	105 GB	$10.86 \cdot 10^{-3}$
1d	3.29 GB	171.4 GB	$19.19 \cdot 10^{-3}$
2a	681 MB	59.0 GB	$11.54 \cdot 10^{-3}$
2b	62.6 GB	143.2 TB	$0.44 \cdot 10^{-3}$

REFERENCES

[1] O. Borries, P. Meincke, E. Jørgensen, and P. C. Hansen, "Multi-level Fast Multipole Method for Higher-Order Discretizations," *IEEE Transactions on Antennas and Propagation*, vol. 62, no. 9, pp. 4695–4705, 2014.

[2] E. Jørgensen, "Higher-Order Integral Equation Methods in Computational Electromagnetics," PhD thesis, ISBN 87-91184-21-5, Technical University of Denmark, Ørsted-DTU, Lyngby, Denmark, May 2003.

[3] ESA, *http://www.esa.int/For_Media/Press_Releases/OLYMPUS_End_of_mission*.

[4] O. Breinbjerg and D. I. Kaklamani, "The Electric Field Integral Equation and the Physical Theory of Diffraction in Scattering Analysis," in *Applied Computational Electromagnetics - State of the Art and Future Trends*. Springer, 1999, pp. 60–111.

[5] K. Pontoppidan, *GRASP Technical Description.*, 2008.

[6] S. M. Rao, D. R. Wilton, and A. W. Glisson, "Electromagnetic scattering by surfaces of arbitrary shape," *IEEE Transactions on Antennas and Propagation*, vol. 30, no. 3, 1982.